

Subwavelength gratings fabricated on semiconductor substrates via E-beam lithography and lift-off method

KIEN WEN SUN^{1,*}, SHIH-CHIEH HUANG², ARA KECHIANTZ¹ AND CHIEN-PING LEE²

¹*Department of Physics, National Dong Hwa University, 1 Da Hseuh Rd., Sec. 2, Shoufeng, Taiwan, Hualien 974, R.O.C.*

²*Department of Electronics Engineering and Institute of Electronics, National Chiao Tung University, Hsin Chu, Taiwan, R.O.C.*

(*author for correspondence: E-mail: kwsun@mail.ndhu.edu.tw)

Received 8 June 2004; accepted 9 February 2005

Abstract. We present results of the fabrication and measurements on reflective polarizers consisting of stacked bi-layer subwavelength metal gratings prepared on GaAs (100) substrates. These linear gratings were fabricated using electron-beam direct-writing lithography and the lift-off method with periods less than the wavelength of light used for measurements. At normal incidence, the polarizer reflects the light polarized perpendicular to the grating lines (transverse magnetic polarization, TM polarized) but absorbs parallel-polarized light (transverse electric polarization, TE polarized). By optimizing structural parameters, the polarization extinction ratio close to 20 has been experimentally achieved at wavelength of 650 nm.

Key words: birefringence, E-beam lithography, polarizer, subwavelength grating

1. Introduction

It has been shown that when a grating is made in an isotropic material with a period much shorter than the wavelength for the light passing or reflected through it can not diffract the light, but the asymmetry introduces a large birefringence (Born and Wolf 1980; Yariv and Yeh 1984; Shiraishi *et al.* 1991; Gluch *et al.* 1992; Raguin and Morris 1993; Grann *et al.* 1994; Campbell and Kostuk 1995). Crystals such as quartz and calcite exhibit birefringence effects from their molecular structures; their birefringence increases linearly with thickness. When a subwavelength grating period is made in a uniaxial material with the grating vector parallel to the optical axis of the material, the total birefringence properties will be enhanced. It has been shown theoretically that the subwavelength grating period introduces much more phase shift from the birefringence than the natural birefringence of the quartz substrate (Han *et al.* 1996). The effective index of refraction for light polarized along

the grooves can also be very different for light polarized perpendicular to the grooves. These birefringent nanostructures can be used to control and rotate the polarization of semiconductor laser devices such as vertical cavity surface-emitting lasers (VCSELs) (Zhuang *et al.* 1996). The birefringence effect could be over two orders of magnitude larger than that of usual birefringent crystals, allowing the waveplates to be much less than a micron thick.

Recently, one-dimensional 280 nm period silicon grating designed to exhibit polarization dependent reflection or antireflection behavior at visible wavelengths has been fabricated and tested in Brundrett *et al.* (1998). More recently, a reflective polarizer consisting of two layers of 190 nm period metal gratings was fabricated on a silica substrate using nanoimprint technology. The polarization extinction ratio of 200 at wavelength of 632.8 nm was achieved and it was attributed to the resonance between the two layers of metal gratings (Deshpande *et al.* 2000). Subwavelength antireflection gratings for GaSb in visible and near-infrared wavelengths were demonstrated by Kanamori *et al.* (2003). At wavelengths ranged from 500 to 2000 nm, the gratings decreased the reflection as much as 5–10% from the original value.

In this study, we demonstrate the design and fabrication of polarizing mirror/absorber based on a subwavelength metal grating on GaAs (100) wafer via electron beam lithography and lift-off method. This device can reflect light polarized perpendicular to the grating grooves and absorb light polarized along the grating grooves. This device operates as a polarizing mirror or absorber at normal incidence for a semiconductor laser diode emitting at a wavelength of 650 nm. Such a compact device could be easily integrated with semiconductor based light emitting devices or replace bulky and costly birefringent crystal prisms.

2. Experimental

Schematics of the fabrication processes used to produce the gratings are shown in Fig. 1. A semi-insulating GaAs wafer was diced into 1 cm^2 substrate, which were clean with a modified RCA clean and then dried at 150°C for 1 h to drive off excess moisture. The fabrication process commences by spinning a 400 nm thick 950 PMMA onto the GaAs wafer using LAURELL coater and prebakes at 90°C for 30 min. Grating patterns were directly written with the electron beam in a square area of about $100 \times 100\ \mu\text{m}$. The exposed sample was developed at 25°C in MIBK:IPA = 1:3 solution followed by residue PMMA descummed through ULVAC Ozone system. In Fig. 2 the scanning electron microscope (SEM) and transmission electron microscope (TEM) images before the gratings were coated with metals are shown. The cross section of the PMMA grating is close to the shape of a rectangle. Finally, after the photoresist gratings were trimmed, a 50 nm thick

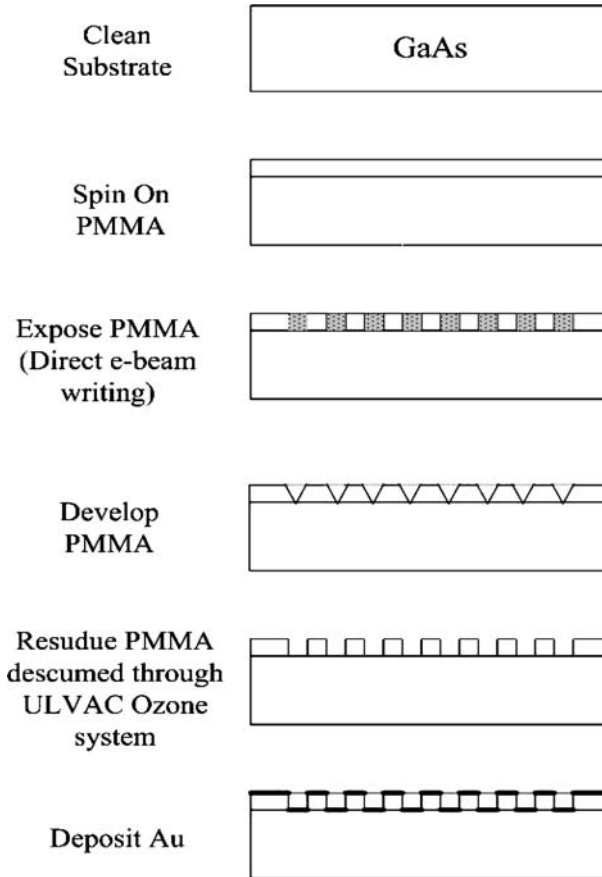


Fig. 1. Fabrication process steps used to produce subwavelength gratings on GaAs (100) substrates.

of Au was evaporated on samples using the ULVAC electron-beam evaporator at a pressure of 2×10^{-6} torr to form the double-layer metal grating structures. At room temperature, the mean free path of the evaporated atoms is well above 100 cm at such a pressure. Therefore, the incoming beam is non-divergent. For a normally incident beam, the sidewalls of the PMMA grating will not be coated.

We fabricated six sets of $100 \times 100 \mu\text{m}$ gold wire grids with a fixed thickness and changed the width of wire and pitch size by varying the dose of the electron beam. Six sets of gratings were prepared with pitch sizes of 145, 225, 260, 310, 360, and 420 nm and top width of 54, 84, 98, 125, 152, and 168 nm, respectively. The dimensions of the fabricated nano-gratings are summarized in Table 1.

In Fig. 3 we show the schematics of our experimental setup. Due to the limited area of gratings, a long-working distance object lens was used to

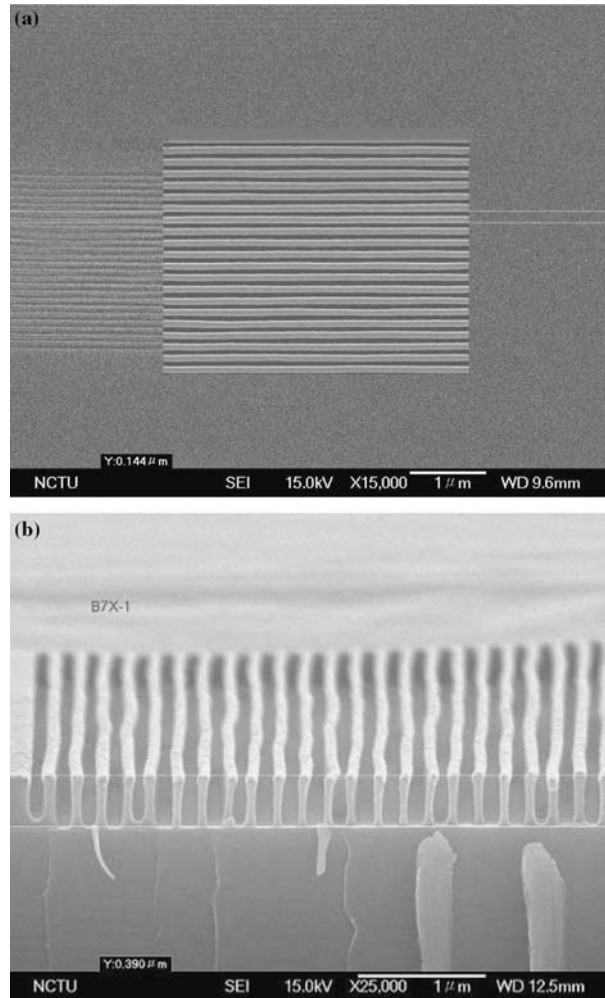


Fig. 2. (a) Scanning electron micrograph and (b) transmission electron micrograph of our bi-layer grating fabricated by electron-beam direct-writing lithography and the lift-off method.

focus the laser beam onto the square area with gratings with a diameter of approximately $30\ \mu\text{m}$ (as shown in Fig. 3). Reflectance measurements for those gratings were done at fixed wavelength of $650\ \text{nm}$ at normal incidence. An AlGaAs semiconductor laser diode served as the light source. The output of the laser diode was either TE or TM polarized by going through a broadband polarizer cube to ensure a linear-polarized incident light. The reflected TE or TM polarized laser beam was measured with the combination of a Si p-i-n photodetector and a current meter. The reflectance is defined as the ratio of the light intensities reflected from the substrates with and without the gratings. The substrates without the gratings $50\ \text{nm}$ thick Au layer and reflects $R_S = 30\%$ of incident light.

Table 1.

Sample number	1	2	3	4	5	6
Pitch size (Λ , nm)	420	360	310	260	225	145
Metal width (nm)	168	152	125	98	84	54

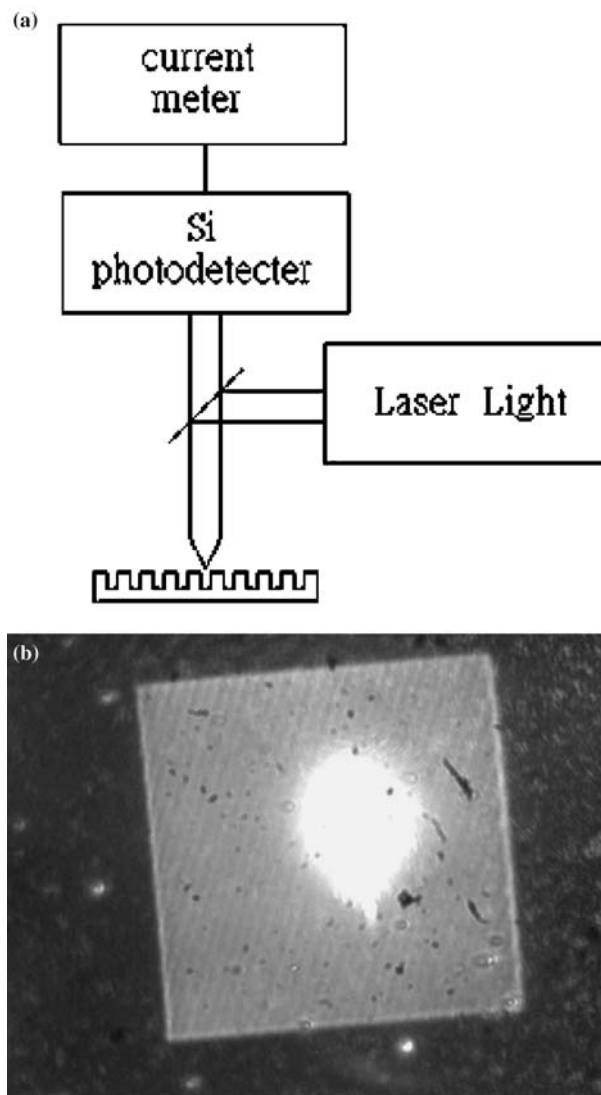


Fig. 3. (a) Schematics of the experimental setup for measuring the reflectance from the subwavelength gratings and (b) the image of the laser spot on the grating area.

3. Results and discussion

The reflectance for both the TM (R_{TM}) and TE (R_{TE}) polarized incident light was recorded and the extinction ratio of $R_{\text{TM}}/R_{\text{TE}}$ is plotted in Fig. 4 for all six different gratings. We find that the extinction ratio increases as the pitch size and the wire width are both decreased at the fixed incident laser wavelength of 650 nm. The extinction ratio of nearly 20 was achieved for the grating with pitch size of 145 nm and top wire width of 54 nm. For this sample, the reflectance of TM polarized light, R_{TM} , is 78%. Hence the losses of this polarizer, $1-R_{\text{S}}R_{\text{TM}}$, are 77%.

The parameters of our gratings' design are depicted in Fig. 5. The bi-layer metal grating considered in this work is completely described by its filling factor F , groove depth d , period Λ , grating vector \mathbf{K} , and the refractive indices n_{a} , n_{m} , n_{p} and n_{s} of its air, metal, PMMA and substrate materials. The grating period Λ is, in general, composed of several regions with different refractive indices. The PMMA grating between the top and bottom metal gratings behaves like a uniaxial birefringent medium; the index of refraction n_{p} for the TE and TM polarization is 1.20 and 1.11, respectively (Moharram *et al.* 1995; Lalanne and Morris 1996). With parameters from the gratings that we have fabricated, we have performed a study of normal incidence reflectance with the rigorous coupled-wave analysis (RCWA) (Moharram *et al.* 1995, Lalanne and Morris 1996). The RCWA method has been the most widely used for the accurate analysis of the diffraction of electromagnetic waves by periodic structures. This RCWA method is also a relatively straightforward technique for calculating the exact solution of Maxwell's equations for the electromagnetic diffraction by grating structures. The general approach for solving the exact electromagnetic-boundary-value problem associated with the diffraction grating is to find solutions that satisfy Maxwell's equation in each of the regions (input, grating, and output) and then match the tangential electric- and magnetic-field components at the boundaries. To simplify the calculation, we only consider the case of planar diffraction. The incident polarization is decomposed into a TE ($\mathbf{E} \perp \mathbf{K}$) and TM ($\mathbf{H} \perp \mathbf{K}$) polarization problem, which are handled independently. The calculated extinction ratios for the 650 nm light polarized parallel to the grooves (TE) and perpendicular to the grooves (TM) are also shown in Fig. 4 for all the six gratings that we fabricated for this experiment. The measured reflectance extinction ratios are approximately half that expected from the calculations. This is partly due to the actual shape of the fabricated gratings is slightly different from an ideal rectangle which was the model we used in the calculations. The filling factor and the groove depth are also not precisely met due to the fluctuation on the width of the actual grating.

The losses of the polarizer are as large as 77% as a result of non-optimal parameters of grating design and, in particular, of as low as 30% reflectivity

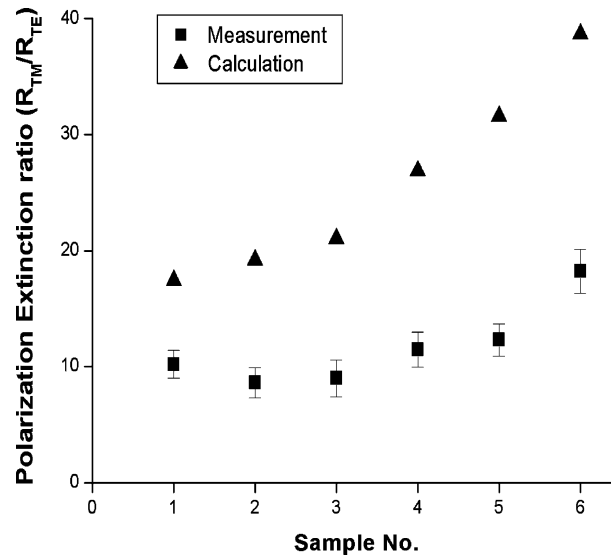


Fig. 4. Measured and calculated polarization extinction ratio (R_{TM}/R_{TE}) for all six samples.

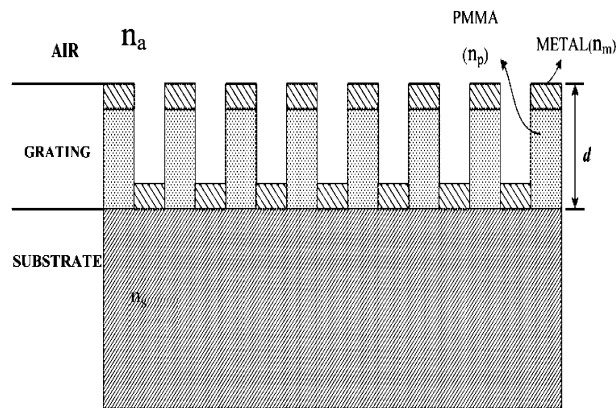


Fig. 5. Bi-layer metal grating geometry showing filling factor F , groove depth d , period Λ , grating vector \mathbf{K} .

of 50 nm thick Au layer. However, the grating fabrication process was limited primarily by non-uniformity at the development step. Further tuning and optimization of the process would improve the controlling of the grating shapes and uniformity. Although our nano-gratings have already achieved polarization extinction ratio of nearly 20, however, with optimization of the metal layer thickness, PMMA thickness, uniformity of grating pitches and shapes, we believe the parameters of polarizer, the extinction ratio and the losses of polarizer, can be improved by an order of magnitude.

4. Conclusions

We have demonstrated subwavelength gratings prepared via the electron-beam lithography and lift-off techniques on GaAs (100) substrates. One of the gratings we fabricated has enhanced the polarized extinction ration to nearly 20 at the incident wavelength of 650 nm. These subwavelength gratings can be directly fabricated and integrated with current semiconductor light sources based on GaAs and Si. Therefore, these nanostructures have the potential for integration with semiconductor photonic devices, including vertical cavity surface emitting lasers, for which they may provide the polarization functionality and control. Not to mention that the fabrication processes are completely compatible with existing semiconductor technology.

Acknowledgements

This work was supported by the National Science Council of Republic of China under contract Grant No. NSC92-2120-E-259-001.

References

- Born, M. and E. Wolf. *Principle of Optics*, Pergamon, New York, 1980.
- Yariv, A. and P. Yeh. *Optical Waves in Crystals, Propagation and Control of Laser Radiation*, Wiley, New York, 1984.
- Shiraishi, K., T. Sato, and S. Kawakami. *Appl. Phys. Lett.* **58** 211, 1991.
- Gluch, E., H. Haidner, P. Kipfer, J.T. Sheridan, and N. Streibl. *Opt. Commun.* **89** 173, 1992.
- Raguin, D.H. and G.M. Morris, *Appl. Opt.* **32**, 2582, 1993.
- Grann, E.B., M.G. Moharam, and D.A. Pommet. *J. Opt. Soc. Am.* **A11** 2695, 1994.
- Campbell, G. and R.K. Kostuk. *J. Opt. Soc. Am.* **A12** 1113, 1995.
- Han, C.W. and R.K. Kostuk. *J. Opt. Soc. Am.* **A13** 1728, 1996.
- Zhuang, L., S. Schablisky, R.C. Shi, and S.Y. Chou. *J. Vac. Sci. Tech.* **B14** 4055, 1996.
- Brundrett, D.L., T.K. Gaylord, and E.N. Glytsis. *Appl. Opt.* **37** 2534, 1998.
- Yu, Z., P. Deshpande, W. Wu, J. Wang, and S.Y. Chou. *Appl. Phys. Lett.* **77** 927, 2000.
- Kanamori, Y., K. Kobayashi, H. Yugami, and K. Hane. *Jpn. J. Appl. Phys.* **42** 4020, 2003.
- Yariv, A. and P. Yeh. *J. Opt. Soc. Am.* **67** 438, 1977.
- Moharram, M.G., E.B. Grann, D.A. Pommet, and T.K. Gaylord. *J. Opt. Soc. Am.* **A12** 1068, 1995.
- Lalanne P. and G.M. Morris. *J. Opt. Soc. Am.* **A13** 779, 1996.